

Finite element approximation of large bending isometries

Sören Bartels

Received: 30 January 2012 / Revised: 11 January 2013 / Published online: 20 February 2013
© Springer-Verlag Berlin Heidelberg 2013

Abstract A finite element scheme for the approximation of large isometric deformations with minimal bending energy is devised and analyzed. The convergence to a stationary point and energy decreasing property of an iterative algorithm for the numerical solution of the scheme is proved. Numerical experiments illustrate the performance of the iteration and show that the discretization leads to accurate approximations for large vertical loads and compressive boundary conditions.

Mathematics Subject Classification (1991) 65N12 · 65N30 · 74K20

1 Introduction

Mathematical models for plate bending have recently been rigorously derived in Ref. [19] via Γ -convergence from three-dimensional elasticity. For $\varepsilon > 0$ let the deformation $y_\varepsilon : \Omega_\varepsilon \rightarrow \mathbb{R}^3$ of the thin domain $\Omega_\varepsilon = \Omega \times (-\varepsilon/2, \varepsilon/2) \subset \mathbb{R}^3$ be a minimizer of the energy functional

$$E_\varepsilon^{3D}(y) = \int_{\Omega_\varepsilon} \widehat{W}(\nabla y) dx - \int_{\Omega_\varepsilon} \widehat{f} \cdot y dx$$

with an appropriate isotropic stored-energy function \widehat{W} , an external force $\widehat{f} : \Omega_\varepsilon \rightarrow \mathbb{R}^3$, and subject to boundary conditions $y_\varepsilon = \widehat{y}_D$ on $\Gamma_D \times (-\varepsilon, \varepsilon)$ for $\Gamma_D \subset \partial\Omega$. Provided that $\varepsilon^{-3} E_\varepsilon^{3D}(y_\varepsilon)$ remains bounded as $\varepsilon \rightarrow 0$ it has been shown that the

S. Bartels (✉)

Abteilung für Angewandte Mathematik, Albert-Ludwigs-Universität Freiburg,
Hermann-Herder Str. 10, 79104 Freiburg i.Br., Germany
e-mail: bartels@ins.uni-bonn.de; bartels@mathematik.uni-freiburg.de

cluster points of solutions $(y_\varepsilon)_{\varepsilon>0}$ for $\varepsilon \rightarrow 0$ are the minimizers of the reduced model

$$E(y) = \int_{\Omega} W(D^2y, \nabla y) dx - \int_{\Omega} f \cdot y dx = \frac{1}{24} \int_{\Omega} (2\mu |II|^2 + \frac{\lambda\mu}{\mu + \lambda/2} (\text{tr} II)^2) dx - \int_{\Omega} f \cdot y dx$$

among smooth isometries $y : \Omega \rightarrow \mathbb{R}^3$ with second fundamental form $II = -(D^2y)b$ whose trace is denoted by $\text{tr} II$ and with normal $b = \partial_1 y \times \partial_2 y$, subject to the conditions $y|_{\Gamma_D} = y_D$ and $b|_{\Gamma_D} = b_D$. The isometry condition means that the first fundamental form $I = (\nabla y)^\top \nabla y$ coincides with the identity matrix I_2 almost everywhere in Ω . The parameters λ and μ are defined through the second derivative of W , the function $f : \Omega \rightarrow \mathbb{R}^3$ is an average of the function \hat{f} in vertical direction, and the boundary data y_D and b_D are defined through \hat{y}_D . This two-dimensional model coincides with the formulation proposed in Ref. [25]. For related lower dimensional theories in different scaling regimes we refer the reader to Ref. [18, 20, 12].

As a consequence of Gauss's *theorema egregium* we have for an isometry $y : \Omega \rightarrow \mathbb{R}^3$ that the Gaussian curvature K vanishes. Therefore, we deduce that for the mean curvature H , which is defined as half the trace of the Weingarten mapping, we have the identity $|II|^2 = 4H^2 - 2K = 4H^2$. Moreover, we have for smooth isometries that $\text{tr} II = 2H$ and $-\Delta y = 2Hb$ and

$$|D^2y|^2 = |II|^2 = 4H^2 = |\text{tr} II|^2 = |\Delta y|^2,$$

cf. Sect. 6.3. The density results for smooth isometries in Ref. [21] therefore allow us to consider the energy functional

$$E(y) = \frac{\alpha}{2} \int_{\Omega} |D^2y|^2 dx - \int_{\Omega} f \cdot y dx$$

among isometries $y : \Omega \rightarrow \mathbb{R}^3$ that satisfy the boundary conditions stated above. The first part of the energy functional coincides with the Willmore energy proposed in Ref. [28] on isometries. We remark that our numerical method is not restricted to the particular form of the energy E and flat isometries but devises a general approach to the approximation of an isometry constraint.

Critical aspects in the numerical minimization of the reduced energy functional E are the occurrence of second order derivatives and the nonlinear pointwise constraint that the deformation $y : \Omega \rightarrow \mathbb{R}^3$ is an isometry, i.e., that the first fundamental form $I = (\nabla y)^\top \nabla y$ satisfies $I = I_2$ with the identity matrix $I_2 \in \mathbb{R}^{2 \times 2}$. Our approach to the iterative minimization of E results from the following steps: We first relax

the second order derivatives by introducing the variable $\Phi \approx \nabla y$, i.e., for a small parameter $t > 0$ we consider

$$E_t(\Phi, y) = \frac{t^{-2}}{2} \|\Phi - \nabla y\|^2 + \frac{\alpha}{2} \int_{\Omega} |\nabla \Phi|^2 dx - \int_{\Omega} f \cdot y dx$$

subject to the boundary conditions $y|_{\Gamma_D} = y_D$, $\Phi|_{\Gamma_D} = \Phi_D$ and the pointwise constraint $\Phi^\top \Phi = I_2$, i.e., the column vectors $\Phi_1, \Phi_2 \in \mathbb{R}^3$ of $\Phi = [\Phi_1, \Phi_2]$ are perpendicular unit-length vector fields that are prescribed on Γ_D . Here we replaced the condition defined through b_D by an equivalent one defined through a matrix-valued function Φ_D whose column vectors satisfy $\Phi_{D,1} \times \Phi_{D,2} = b_D$, cf. Remark 2.1 (i) below. Notice that the functional E_t is convex and that the space of admissible pairs (Φ, y) is non-empty provided that y_D and Φ_D admit appropriate extensions to Ω . The fact that the original problem may have no solutions, i.e., that the set of admissible deformations may be empty, is related to the possibility that the minimal values of the energies $(E_t)_{t>0}$ may be unbounded as t tends to zero. We remark that even if a minimizer for E exists, the Euler–Lagrange equations may not hold, e.g., for the fully clamped plate described by $y_D(x) = (x, 0)^\top$ and $b_D(x) = (0, 0, 1)^\top$ for $x \in \Gamma_D = \partial\Omega$ the only admissible isometry equals y_D .

For the minimization of E_t we employ a discrete H^1 gradient flow of E_t with respect to Φ , i.e., we consider the time-incremental evolution defined by the successive minimization of the functionals

$$E_t^n(\Phi, y) = \frac{1}{2\tau} \|\nabla(\Phi - \Phi^{n-1})\|^2 + \frac{t^{-2}}{2} \|\Phi - \nabla y\|^2 + \frac{\alpha}{2} \int_{\Omega} |\nabla \Phi|^2 dx - \int_{\Omega} f \cdot y dx,$$

where Φ^{n-1} is the solution from the previous time step and $\tau > 0$ the time-step size. The iteration may be regarded as an H^2 flow of the functional E and is justified by the fact that E is finite only on deformations $y \in H^2(\Omega; \mathbb{R}^3)$. Motivated by work in Ref. [1, 6, 3] the condition that Φ satisfies $\Phi^\top \Phi = I_2$ is in the minimization of E_t^n replaced by its linearization about Φ^{n-1} , i.e., by

$$(\Phi - \Phi^{n-1})^\top \Phi^{n-1} + \Phi^{n-1, \top} (\Phi - \Phi^{n-1}) = 0.$$

This means that for the two column vectors of $\Phi = [\Phi_1, \Phi_2]$ and $\Phi^{n-1} = [\Phi_1^{n-1}, \Phi_2^{n-1}]$ we impose that

$$(\Phi_1 - \Phi_1^{n-1}) \cdot \Phi_1^{n-1} = 0, \quad (\Phi_2 - \Phi_2^{n-1}) \cdot \Phi_2^{n-1} = 0$$

and

$$(\Phi_1 - \Phi_1^{n-1}) \cdot \Phi_2^{n-1} + (\Phi_2 - \Phi_2^{n-1}) \cdot \Phi_1^{n-1} = 0$$

The new approximation Φ^n is obtained from a correction of the minimizer $\tilde{\Phi}^n$ of E_t^n , i.e., we set

$$\Phi_1^n = \frac{\tilde{\Phi}_1^n}{|\tilde{\Phi}_1^n|}, \quad \Phi_2^n = \frac{\tilde{\Phi}_2^n}{|\tilde{\Phi}_2^n|}.$$

Notice that $|\tilde{\Phi}_j^n|^2 = |\Phi_j^{n-1}|^2 + |\tilde{\Phi}_j^n - \Phi_j^{n-1}|^2$ for $j = 1, 2$ so that if $|\Phi_j^{n-1}| = 1$ then the projection onto the unit sphere is well defined. Moreover, the projection of the vectors $\tilde{\Phi}_1^n$ and $\tilde{\Phi}_2^n$ will not change their relative angle and the identity

$$\tilde{\Phi}_1^n \cdot \tilde{\Phi}_2^n = \Phi_1^{n-1} \cdot \Phi_2^{n-1} + (\tilde{\Phi}_1^n - \Phi_1^{n-1}) \cdot (\tilde{\Phi}_2^n - \Phi_2^{n-1})$$

together with the observation that the second term on the right-hand side is of higher order allow us to employ an inductive argument to show that $\Phi_1^n \cdot \Phi_2^n$ remains small. We will show that a discretization of this iteration with low order finite elements on a weakly acute triangulation is energy decreasing and converges to a stationary point of the discrete energy $E_{h,t}$ under the mild constraint on the time-step size

$$\tau \leq Ct.$$

The limiting stationary point may not be a global minimizer but in our numerical experiments we did not observe problems related to local minima.

The spatial discretization of the functionals E_t^n will be based on a continuous extension of a robust mixed method for Reissner–Mindlin plates proposed and analyzed in Ref. [2] which is uniformly accurate and optimally convergent for $0 < t \leq 1$ and small vertical displacements. Moreover, this method allows for an efficient solution of the discrete systems of equations. It realizes a softening of the term $(t^{-2}/2)\|\Phi - \nabla y\|^2$ and leads to system matrices whose inverses are uniformly bounded in t as long as the displacement is small and exterior forces act in vertical direction.

The finite element approximation of bending problems such as the minimization of the Willmore energy has recently attracted significant attention motivated by applications in biophysics and computer graphics, cf. [11, 15, 14, 13, 4, 27, 16, 5, 8, 17]. The method developed in Ref. [27] replaces the Willmore functional by a discrete quadratic curvature energy that can be regarded as a discretization of Δy with Crouzeix–Raviart finite elements and imposes an isometry condition by requiring that the lengths and the angles of edges in the underlying triangulation remain (approximately) unchanged by the discrete deformation. The method can only lead to good approximations of the continuous solutions if the directions of the edges are uniformly distributed. In general, mesh-dependence of the approximations has to be expected. The algorithms devised in Ref. [5, 8, 17] approximate solutions of the Willmore flow by computing a family of discrete closed surfaces, employing the identity $-2Hb = \Delta_\Gamma \text{id}_\Gamma$ on Γ , and incorporating the constraint that the surface area remains constant. Most algorithms that evolve the surface instead of computing a family of parametrizations have to deal with problems related to emerging mesh irregularities. An approach to the approximation of bending isometries based on discrete Kirchhoff triangles has recently been investigated by the author in Ref. [7].

Using an isometry constraint in large bending problems has several advantages: (i) computationally, it allows us to work on one fixed grid which avoids difficulties related to mesh distortions, (ii) analytically, the condition is the result of rigorous derivations of lower dimensional theories from three-dimensional elasticity which imply existence of solutions, and (iii) physically, it seems more meaningful since it is a local condition and therefore appears better suited than a global constraint for the

modeling of thin incompressible elastic solid sheets. To our knowledge, the proposed finite element method is the first one that approximates an isometry constraint and allows free boundary conditions on part of the boundary of the plate. In addition, we provide a complete numerical analysis for the discretization and the iterative scheme that solves the discrete formulation.

The outline of this paper is as follows. In Sect. 2 we recall a few facts about the considered mathematical model and the employed mixed finite element method. Section 3 provides a Γ -convergence result for the discretized functional which implies convergence of numerical approximations provided that smooth isometries are dense in the set of admissible deformations or that there exists a minimizer $\bar{y} \in H^3(\Omega; \mathbb{R}^3)$. Sufficient conditions for the convergence of the discretized H^2 gradient flow to stationary points are derived in Sect. 4 and its efficient implementation is discussed in Sect. 5. Numerical experiments with vertical loads and compressive boundary conditions are reported in Sect. 6. Some auxiliary results are proved in Sect. 6.3.

2 Preliminaries

2.1 Notation

Throughout this paper we abbreviate the L^2 norm on Ω by $\|\cdot\|$ and let (\cdot, \cdot) be the L^2 inner product on Ω . By $|\cdot|$ we denote the Frobenius norm of a matrix or a vector. For a scalar function ϕ we define the vectorial curl operator by $\text{Curl}\phi = (-\partial_2\phi, \partial_1\phi)$ and for a vector field $v : \Omega \rightarrow \mathbb{R}^3$ we define $\text{Curl}v : \Omega \rightarrow \mathbb{R}^{3 \times 2}$ by applying the curl operator to each component of v . We use standard notation for Lebesgue and Sobolev spaces. We always let C denote a generic nonnegative constant that is independent of discretization parameters.

2.2 Mathematical model

For a bounded Lipschitz domain $\Omega \subset \mathbb{R}^2$ with polygonal boundary, a function $f \in L^2(\Omega; \mathbb{R}^3)$, and functions $y_D, b_D \in L^2(\Gamma_D; \mathbb{R}^3)$ on a closed subset $\Gamma_D \subset \partial\Omega$ of positive surface measure and such that y_D has a tangential derivative $\partial y_D / \partial s \in L^2(\Gamma_D; \mathbb{R}^3)$ along Γ_D with $|\partial y_D / \partial s| = 1$ and $|b_D| = 1$, the functional $E : H^1(\Omega; \mathbb{R}^3) \rightarrow \mathbb{R} \cup \{+\infty\}$ is finite for deformations in

$$\mathcal{A} = \{z \in H^2(\Omega; \mathbb{R}^3) : (\nabla z)^\top \nabla z = I_2, z|_{\Gamma_D} = y_D, (\partial_1 z \times \partial_2 z)|_{\Gamma_D} = b_D\}$$

and is for $y \in \mathcal{A}$ defined by

$$E(y) = \frac{\alpha}{2} \int_{\Omega} |D^2 y|^2 dx - \int_{\Omega} f \cdot y dx.$$

We assume that $\mathcal{A} \neq \emptyset$ in the following.

- Remark 2.1** (i) The boundary condition $b|_{\Gamma_D} = b_D$ can be replaced by the condition $\nabla y|_{\Gamma_D} = \Phi_D$, where $\Phi_D \in L^2(\Gamma_D; \mathbb{R}^{3 \times 2})$ is uniquely defined through the conditions $\Phi_D^\top \Phi_D = I_2$, $\Phi_D \theta = \partial y_D / \partial s$ for the unit tangent vector θ on Γ_D , and $\Phi_{D,1} \times \Phi_{D,2} = b_D$.
- (ii) The set of admissible displacements \mathcal{A} may be empty in general and compatibility of y_D and b_D is required to guarantee $\mathcal{A} \neq \emptyset$.

We assume that the functions y_D and Φ_D admit smooth extensions to Ω and are sufficiently smooth so that they can be approximated with arbitrary accuracy in $L^2(\Gamma_D)$ by nodal interpolation on Γ_D . We will also use that smooth isometries are dense in \mathcal{A} which is justified by results in Ref. [26, 21, 23]. Since a precise formulation of the conditions on the domain and boundary data is technical, we formulate the result as an assumption. The use of this result can be avoided if there exists a minimizer $\bar{y} \in H^3(\Omega; \mathbb{R}^3) \cap \mathcal{A}$ of E . We refer the reader to Ref. [22] for related regularity results.

Assumption (D). For all $z \in \mathcal{A}$ and $\varepsilon > 0$ there exists $z_\varepsilon \in C^\infty(\bar{\Omega}; \mathbb{R}^3) \cap \mathcal{A}$ with $\|D^2(z - z_\varepsilon)\| \leq \varepsilon$.

Remark 2.2 Assumption (D) is satisfied for rectangular plates whose deformation and deformation gradient are prescribed on one or two opposite sides by rigid body motions that lead to a non-empty set of admissible deformations \mathcal{A} , cf. [22, 24].

2.3 Finite element spaces

For a regular triangulation \mathcal{T}_h of the domain Ω with maximal mesh-size $h > 0$ let \mathcal{N}_h denote the set of nodes (vertices of elements) and \mathcal{E}_h the set of edges of elements. For each $E \in \mathcal{E}_h$ let z_E denote the midpoint of the edge E and for each $T \in \mathcal{T}_h$ let z_T be the midpoint of the triangle T . We define the finite element spaces

$$\begin{aligned}\mathcal{L}^0(\mathcal{T}_h) &= \{\phi_h \in L^1(\Omega) : \phi_h|_T \text{ constant for all } T \in \mathcal{T}_h\}, \\ \mathcal{S}^1(\mathcal{T}_h) &= \{\phi_h \in C(\bar{\Omega}) : \phi_h|_T \text{ affine for all } T \in \mathcal{T}_h\}, \\ \mathcal{S}_{cr}^1(\mathcal{T}_h) &= \{\phi_h \in L^1(\Omega) : \phi_h|_T \text{ affine for all } T \in \mathcal{T}_h \\ &\quad \text{and } \phi_h \text{ continuous at every } z_E, E \in \mathcal{E}_h\}.\end{aligned}$$

With the nodal basis $(\varphi_z : z \in \mathcal{N}_h)$ the bubble function associated to an element $T \in \mathcal{T}_h$ with vertices $z_1, z_2, z_3 \in \mathcal{N}_h$ is defined by $b_T = \varphi_{z_1}\varphi_{z_2}\varphi_{z_3}$ and we set

$$\mathcal{B}^3(\mathcal{T}_h) = \left\{ \phi_h = \sum_{T \in \mathcal{T}_h} \alpha_T b_T : (\alpha_T)_{T \in \mathcal{T}_h} \subset \mathbb{R} \right\}.$$

We let $P_0 : L^2(\Omega) \rightarrow \mathcal{L}^0(\mathcal{T}_h)$ denote the L^2 projection onto $\mathcal{L}^0(\mathcal{T}_h)$ and $\mathcal{I}_h : C(\bar{\Omega}) \rightarrow \mathcal{S}^1(\mathcal{T}_h)$ the nodal interpolation operator. We remark that for $v_h \in \mathcal{S}^1(\mathcal{T}_h)$ and $b_h \in \mathcal{B}^3(\mathcal{T}_h)$ we have

$$(\nabla v_h, \nabla b_h) = 0. \quad (2.1)$$

For every $v_h \in \mathcal{S}^1(\mathcal{T}_h)$ and $1 \leq p < \infty$ we have the equivalence

$$C^{-1} \|v_h\|_{L^p(\Omega)}^p \leq \sum_{z \in \mathcal{N}_h} h_z^d |v_h(z)|^p \leq C \|v_h\|_{L^p(\Omega)}^p. \quad (2.2)$$

We will occasionally employ inverse estimates of the form

$$\|\nabla v_h\| \leq Ch^{-1} \|v_h\|$$

which hold for all $v_h \in \mathcal{S}^1(\mathcal{T}_h)$ and all $v_h \in \mathcal{B}^3(\mathcal{T}_h)$ provided that \mathcal{T}_h is quasiuniform. We say that \mathcal{T}_h is weakly acute if for every interior edge the sum of opposite angles does not exceed π and for every edge on the boundary the angle opposite to it is bounded by $\pi/2$. In this case we have for every $\tilde{v}_h \in \mathcal{S}^1(\mathcal{T}_h)$ with $|\tilde{v}_h(z)| \geq 1$ for all $z \in \mathcal{N}_h$ and $v_h \in \mathbb{V}_{p1}$ defined by $v_h(z) = \tilde{v}_h(z)/|\tilde{v}_h(z)|$ for all $z \in \mathcal{N}_h$ that

$$\|\nabla v_h\| \leq \|\nabla \tilde{v}_h\|. \quad (2.3)$$

We refer the reader to Ref. [6] and Appendix A.2 for a proof.

2.4 Discrete vector fields

Spaces of discrete vector fields are defined by setting

$$\begin{aligned} \mathbb{V}_{p1} &= \mathcal{S}^1(\mathcal{T}_h)^3, & \mathbb{V}_{p1, D} &= \{v_h \in \mathbb{V}_{p1} : v_h|_{\Gamma_D} = 0\}, \\ \mathbb{V}_{cr} &= \mathcal{S}_{cr}^1(\mathcal{T}_h)^3, & \mathbb{V}_{cr, D} &= \{v_h \in \mathbb{V}_{cr} : v_h(z_E) = 0 \text{ for all } E \in \mathcal{E}_h \cap \Gamma_D\}, \\ \mathbb{V}_{mini} &= \mathcal{S}^1(\mathcal{T}_h)^3 \oplus \mathcal{B}^3(\mathcal{T}_h)^3, & \mathbb{V}_{mini, D} &= \{v_h \in \mathbb{V}_{mini} : v_h|_{\Gamma_D} = 0\}, \\ \mathbb{V}_B &= \mathcal{B}^3(\mathcal{T}_h)^3 \end{aligned}$$

and, with ν denoting the outer unit normal to Ω on $\Gamma_N = \partial\Omega \setminus \Gamma_D$,

$$\mathring{\mathbb{Q}}_{p1, N} = \{q_h \in \mathcal{S}^1(\mathcal{T}_h)^3 : (q_h, 1) = 0, (\text{Curl} q_h)\nu = 0 \text{ on } \Gamma_N\}.$$

Given $\Psi_h \in \mathbb{V}_{mini}^2$ we define

$$\mathbb{W}_{mini, D}[\Psi_h] = \{\Phi_h \in \mathbb{V}_{mini, D}^2 : \Phi_h(z)^\top \Psi_h(z) + \Psi_h(z)^\top \Phi_h(z) = 0 \text{ for all } z \in \mathcal{N}_h\},$$

where a pair of vectors $V_1, V_2 \in \mathbb{R}^3$ is identified with the matrix $[V_1, V_2] \in \mathbb{R}^{3 \times 2}$. We note that for every $v_h \in \mathbb{V}_{mini}$ we have $v_h = \mathcal{I}_h v_h + \mathcal{I}_B v_h$ with $\mathcal{I}_h v_h \in \mathbb{V}_{p1}$ and $\mathcal{I}_B v_h \in \mathbb{V}_B$, where

$$\mathcal{I}_B v_h = (1 - \mathcal{I}_h) v_h.$$

2.5 Discontinuous finite element functions

For a (possibly discontinuous) function $v_h \in \mathcal{S}_{cr}^1(\mathcal{T}_h)$ its elementwise gradient $\nabla_h v_h$ is for every $T \in \mathcal{T}_h$ defined by

$$\nabla_h v_h|_T = \nabla(v_h|_T).$$

The interpolation operator $\mathcal{I}_{h,cr} : H^2(\Omega) \rightarrow \mathcal{S}_{cr}^1(\mathcal{T}_h)$ defined by $\mathcal{I}_{h,cr}u(z_E) = u(z_E)$ for all $E \in \mathcal{E}_h$ satisfies

$$\|u - \mathcal{I}_{h,cr}u\| + h\|\nabla u - \nabla_h \mathcal{I}_{h,cr}u\| \leq ch^2\|D^2u\| \quad (2.4)$$

for all $u \in H^2(\Omega)$. We note that we may extend the definition of ∇_h to elementwise weakly differentiable functions and then we have $\nabla_h u = \nabla u$ for every $u \in H^1(\Omega)$. The following lemma shows that bounded sequences of finite element functions in \mathbb{V}_{cr} accumulate at functions in $H^1(\Omega; \mathbb{R}^3)$. A proof is given in Appendix A.3.

Lemma 2.1 *For each $h > 0$ let $y_h \in \mathbb{V}_{cr}$ be such that $y_h(z_E) = y_D(z_E)$ for all $E \in \mathcal{E}_h$ with $E \subset \Gamma_D$ and $\|\nabla_h y_h\| \leq C$. Then there exists $y \in H^1(\Omega; \mathbb{R}^3)$ with $y|_{\Gamma_D} = y_D$ such that (for a subsequence) we have $y_h \rightharpoonup y$ in L^2 and $\nabla_h y_h \rightharpoonup \nabla y$ in L^2 .*

3 Convergence of approximations

Let

$$\begin{aligned} \mathcal{A}_h = \{(\Psi_h, z_h) \in \mathbb{V}_{mini}^2 \times \mathbb{V}_{cr} : \Psi_h(z) = \Phi_D(z) \text{ f.a. } z \in \mathcal{N}_h \cap \Gamma_D, \Psi_h(z)^\top \Psi_h(z) \\ = I_2 \text{ f.a. } z \in \mathcal{N}_h, z_h(z_E) = y_D(z_E) \text{ f.a. } E \in \mathcal{E}_h \cap \Gamma_D\} \end{aligned}$$

and for $t > 0$ and $(\Psi_h, z_h) \in \mathcal{A}_h$ consider the energy functional

$$E_{h,t}(\Psi_h, z_h) = \frac{t^{-2}}{2} \|P_0 \Psi_h - \nabla_h z_h\|^2 + \frac{\alpha}{2} \int_{\Omega} |\nabla \Psi_h|^2 dx - \int_{\Omega} f \cdot z_h dx.$$

Remark 3.1 (i) The use of the projection operator P_0 allows a discrete Helmholtz decomposition of $t^{-2}(P_0 \Phi_h - \nabla_h y_h)$ and is required for the robust solvability of the problem for small displacements with vertical loads, cf. Sect. 5.

(ii) Notice that if y_D and Φ_D are piecewise continuous then we have $\mathcal{A}_h \neq \emptyset$.

Proposition 3.1 (Existence) *If $\mathcal{A}_h \neq \emptyset$ then there exists a minimizer $(\Phi_h, y_h) \in \mathcal{A}_h$ for $E_{h,t}$ with $\|\nabla_h y_h\| \leq C(1 + \|P_0 \Phi_h\|)$.*

Proof For every fixed Ψ_h the minimal $y_h = \mathcal{R}_h \Psi_h$ of $y_h \mapsto E_{h,t}(\Psi_h, y_h)$ among $y_h \in \mathbb{V}_{cr}$ such that the pair $(\Psi_h, y_h) \in \mathcal{A}_h$ satisfies

$$(\nabla_h y_h, \nabla_h z_h) = t^2(f, z_h) + (P_0 \Psi_h, \nabla_h z_h)$$

for all $z_h \in \mathbb{V}_{cr,D}$. Choosing $z_h = y_h - \mathcal{I}_{cr} \tilde{y}_D$ for a continuous extension \tilde{y}_D of y_D yields that

$$\|\nabla_h y_h\| \leq C(1 + \|P_0 \Psi_h\|).$$

For the functional $F_{h,t}(\Psi_h) = E_{h,t}(\Psi_h, \mathcal{R}_h \Psi_h)$ we thus have for every $\delta > 0$ that

$$F_{h,t}(\Psi_h) \geq (\alpha/2) \|\nabla \Psi_h\|^2 - C_\delta \|f\|^2 - \delta \|P_0 \Psi_h\|^2 - C,$$

i.e., $F_{h,t}$ is coercive and hence there exists a minimizer Φ_h such that $(\Phi_h, \mathcal{R}_h \Phi_h) \in \mathcal{A}_h$. \square

Proposition 3.2 (Lower bound) *Let $t = t(h) \rightarrow 0$ as $h \rightarrow 0$ and for each $h > 0$ let $(\Phi_h, y_h) \in \mathcal{A}_h$ with $\|\nabla_h y_h\| \leq C(1 + \|P_0 \Phi_h\|)$ be such that as $h \rightarrow 0$ we have*

$$E_{h,t}(\Phi_h, y_h) \leq C.$$

Then, the sequence $(\Phi_h, y_h)_{h>0}$ has weak accumulation points in $H^1(\Omega; \mathbb{R}^{3 \times 2}) \times H^1(\Omega; \mathbb{R}^3)$ and for each such point $(\Phi, y) \in H^1(\Omega; \mathbb{R}^{3 \times 2}) \times H^1(\Omega; \mathbb{R}^3)$ we have $\Phi = \nabla y$ in Ω , $y \in \mathcal{A}$, and

$$E(y) \leq \liminf_{h \rightarrow 0} E_{h,t}(\Phi_h, y_h).$$

Proof Following the proof of Proposition 3.1 the boundedness $E_{h,t}(\Phi_h, y_h) \leq C$ and $\|\nabla_h y_h\| \leq C(1 + \|P_0 \Psi_h\|)$ imply that $(\Phi_h)_{h>0}$ is bounded in H^1 and thus has weak accumulation points. From the elementwise application of a Poincaré inequality it follows that $P_0 \Phi_h - \Phi_h \rightarrow 0$ in L^2 . Moreover, $(\nabla_h y_h)_{h>0}$ is bounded in L^2 and we deduce with Lemma 2.1 that (after extraction of a subsequence) $\nabla_h y_h \rightharpoonup \nabla y$ in L^2 as $h \rightarrow 0$ with $y|_{\Gamma_D} = y_D$. Let $\Phi \in H^1(\Omega; \mathbb{R}^{3 \times 2})$ be a weak accumulation point of $(\Phi_h)_{h>0}$ in $H^1(\Omega; \mathbb{R}^{3 \times 2})$. By weak continuity of the trace operator we have $\Phi|_{\Gamma_D} = \Phi_D$. The sequence $\Phi_h - \nabla_h y_h$ converges strongly to zero in L^2 so that $\nabla y = \Phi$. Since $\Phi_h(z)^\top \Phi_h(z) = I_2$ for all $z \in \mathcal{N}_h$ we have for every element $T \in \mathcal{T}_h$ by nodal interpolation and inverse estimates with $h_T = \text{diam}(T)$ that

$$\begin{aligned} \|\Phi_h^\top \Phi_h - I_2\|_{L^2(T)} &= \|\Phi_h^\top \Phi_h - \mathcal{I}_h[\Phi_h^\top \Phi_h]\|_{L^2(T)} \leq ch_T^2 \|D^2[\Phi_h^\top \Phi_h]\|_{L^2(T)} \\ &\leq ch_T \|\nabla[\Phi_h^\top \Phi_h]\|_{L^2(T)}. \end{aligned}$$

Discrete norm equivalences show that we have the same estimate in $L^1(T)$ and therefore

$$\begin{aligned} \|\Phi_h^\top \Phi_h - I_2\|_{L^1(\Omega)} &\leq ch \sum_{T \in \mathcal{T}_h} \|\nabla[\Phi_h^\top \Phi_h]\|_{L^1(T)} \leq ch \sum_{T \in \mathcal{T}_h} \|\Phi_h\|_{L^2(T)} \|\nabla \Phi_h\|_{L^2(T)} \\ &\leq ch \|\Phi_h\| \|\nabla \Phi_h\|. \end{aligned}$$

This implies $\Phi^\top \Phi = I_2$ in Ω . In particular, we find that $y \in H^2(\Omega; \mathbb{R}^3)$ is an isometry. The weak lower semicontinuity of the H^1 seminorm implies the assertion of the proposition. \square

Proposition 3.3 (Attainment) *Assume that Assumption (D) holds, let $y \in \mathcal{A}$, and suppose that $t^{-1}h \rightarrow 0$ as $h \rightarrow 0$. For every $h > 0$ there exists a pair $(\Phi_h, y_h) \in \mathcal{A}_h$ such that as $h \rightarrow 0$ we have*

$$E_{h,t}(\Phi_h, y_h) \rightarrow E(y).$$

Proof Owing to Assumption (D) we may assume that $y \in H^3(\Omega)$. Choosing $y_h = \mathcal{I}_{h,cr} y$ and $\Phi_h = \mathcal{I}_h[\nabla y] \in \mathbb{V}_{p1}^2$ we have $(\Phi_h, y_h) \in \mathcal{A}_h$ and owing to standard interpolation results, cf. [9] and (2.4),

$$\begin{aligned} & \|\Phi_h - \nabla y\| + h\|\nabla \Phi_h - D^2 y\| + h\|\Phi_h - \nabla y\|_{L^\infty(\Omega)} + \|y_h - y\| \\ & + h\|\nabla_h y_h - \nabla y\| \leq ch^2\|y\|_{H^3(\Omega)}. \end{aligned}$$

To show that $E_{h,t}(\Phi_h, y_h) \rightarrow E(y)$ we first note that

$$\begin{aligned} t^{-1}\|P_0\Phi_h - \nabla_h y_h\| & \leq t^{-1}(\|P_0\Phi_h - \Phi_h\| + \|\Phi_h - \nabla y\| + \|\nabla_h y_h - \nabla y\|) \\ & \leq Ct^{-1}(h + h^2 + h). \end{aligned}$$

With $\Phi = \nabla y$ it follows that

$$\int_{\Omega} |\nabla \Phi_h|^2 dx \rightarrow \int_{\Omega} |D^2 y|^2 dx$$

as $h \rightarrow 0$. Since we also have that $\int_{\Omega} f \cdot y_h dx \rightarrow \int_{\Omega} f \cdot y dx$ we deduce the assertion. \square

Remark 3.2 (i) For the case that E has a minimizer $\bar{y} \in H^3(\Omega) \cap \mathcal{A}$ we have proved the one-sided error estimate

$$\min_{\mathcal{A}_h} E_{h,t} - \min_{\mathcal{A}} E \leq C(t^{-2}h^2 + h)$$

which motivates the choice $t = \mathcal{O}(h^{1/2})$.

- (ii) Noting that the L^2 projection $\Pi_h : H^1(\Omega) \rightarrow \mathcal{S}^1(\mathcal{T}_h)$ satisfies $\|v - \Pi_h v\| = o(h)$ for every $v \in H^1(\Omega)$ the condition $t^{-1}h \rightarrow 0$ can be replaced by $t^{-1}h \leq C$, i.e., $h = \mathcal{O}(t)$.

The propositions imply the following convergence result.

Theorem 3.1 (Approximation) *Assume that Assumption (D) holds or that E has a minimizer $\bar{y} \in H^3(\Omega; \mathbb{R}^3) \cap \mathcal{A}$. For each $(h, t) > 0$ let $(\Phi_h, y_h) \in \mathcal{A}_h$ be such that $\|\nabla_h y_h\| \leq C(1 + \|P_0\Phi_h\|)$ and*

$$E_{h,t}(\Phi_h, y_h) \leq \min_{(\Psi_h, z_h) \in \mathcal{A}_h} E_{h,t}(\Psi_h, z_h) + \varepsilon_h \leq C$$

where $\varepsilon_h \rightarrow 0$ as $h \rightarrow 0$. Then, if $t^{-1}h \rightarrow 0$ as $h \rightarrow 0$ the sequence $(\Phi_h, y_h)_{h>0}$ has weak accumulation points in $H^1(\Omega; \mathbb{R}^{3 \times 2}) \times H^1(\Omega; \mathbb{R}^3)$ and for each such point $(\Phi, y) \in H^1(\Omega; \mathbb{R}^{3 \times 2}) \times H^1(\Omega; \mathbb{R}^3)$ we have $\Phi = \nabla y$ in Ω , $y \in \mathcal{A}$, and

$$E(y) = \min_{z \in \mathcal{A}} E(z) = \lim_{h \rightarrow 0} E_{h,t}(\Phi_h, y_h).$$

4 Iterative energy reduction

We propose the following scheme for the computation of stationary points of the functional $E_{h,t}$.

4.1 Iterative algorithm

For given $\Phi_h^0 \in \mathbb{V}_{mini}^2$ such that $\Phi_h^0(z) = \Phi_D(z)$ for all $z \in \mathcal{N}_h \cap \Gamma_D$ and $\Phi_h^0(z)^\top \Phi_h^0(z) = I_2$ for all $z \in \mathcal{N}_h$ we iterate the following steps.

Step A. Compute for given $\Phi_h^{n-1} \in \mathbb{V}_{mini}^2$ the pair $(\tilde{\Phi}_h^n, \tilde{y}_h^n) \in \mathbb{V}_{mini}^2 \times \mathbb{V}_{cr}$ with $\tilde{y}_h^n(z_E) = y_D(z_E)$ for all $E \in \mathcal{E}_h \cap \Gamma_D$, $\tilde{\Phi}_h^n(z) = \Phi_D(z)$ for all $z \in \mathcal{N}_h \cap \Gamma_D$, and

$$(\tilde{\Phi}_h^n(z) - \Phi_h^{n-1}(z))^\top \Phi_h^{n-1}(z) + \Phi_h^{n-1}(z)^\top (\tilde{\Phi}_h^n(z) - \Phi_h^{n-1}(z)) = 0$$

that is minimal for

$$\begin{aligned} (\Phi_h, y_h) \mapsto & \frac{1}{2\tau} \left\| \nabla(\Phi_h - \Phi_h^{n-1}) \right\|^2 + \frac{t^{-2}}{2} \left\| P_0 \Phi_h - \nabla_h y_h \right\|^2 \\ & + \frac{\alpha}{2} \int_{\Omega} |\nabla \Phi_h|^2 dx - \int_{\Omega} f \cdot y_h dx. \end{aligned}$$

Step B. Define $\Phi_h^n = \mathcal{I}_B \tilde{\Phi}_h^n + \hat{\Phi}_h^n \in \mathbb{V}_{mini}^2$, where $\hat{\Phi}_h^n \in \mathbb{V}_{p1}^2$ is defined by setting

$$\hat{\Phi}_{h,1}^n(z) = \frac{\tilde{\Phi}_{h,1}(z)}{|\tilde{\Phi}_{h,1}(z)|}, \quad \hat{\Phi}_{h,2}^n(z) = \frac{\tilde{\Phi}_{h,2}(z)}{|\tilde{\Phi}_{h,2}(z)|}$$

for all $z \in \mathcal{N}_h$, and let $y_h^n \in \mathbb{V}_{cr}$ be such that $y_h^n(z_E) = y_D(z_E)$ for all $E \in \mathcal{E}_h \cap \Gamma_D$ and

$$(\nabla_h y_h^n, \nabla_h z_h) = (P_0 \Phi_h^n, \nabla_h z_h) + t^2(f, z_h)$$

for all $z_h \in \mathbb{V}_{cr,D}$.

Remark 4.1 (i) Notice that the part of $\tilde{\Phi}_h^n$ belonging to \mathbb{V}_B^2 remains unchanged in Step B, i.e., only the nodal values are projected onto the unit sphere.

- (ii) The iterates do not satisfy $\Phi_{h,1}^n(z) \cdot \Phi_{h,2}^n(z) = 0$ for $z \in \mathcal{N}_h$ but this quantity remains small.
- (iii) For each $n \geq 1$ there exists a unique solution $(\tilde{\Phi}_h^n, \tilde{y}_h^n)$ in Step A which is the solution of

$$\begin{aligned} & \tau^{-1}(\nabla[\tilde{\Phi}_h^n - \Phi_h^n], \nabla \Psi_h) + t^{-2}(P_0 \tilde{\Phi}_h^n - \nabla_h \tilde{y}_h^n, \Psi_h - \nabla_h z_h) + \alpha(\nabla \tilde{\Phi}_h^n, \nabla \Psi_h) \\ & = (f, z_h) \end{aligned}$$

for all $(\Psi_h, z_h) \in \mathbb{V}_{mini,D}^2 \times \mathbb{V}_{cr,D}$ with

$$(\Psi_h(z) - \Phi_h^{n-1}(z))^\top \Phi_h^{n-1}(z) + \Phi_h^{n-1}(z)^\top (\Psi_h(z) - \Phi_h^{n-1}(z)) = 0 \quad (4.1)$$

for all $z \in \mathcal{N}_h$. In particular, we have for all $z_h \in \mathbb{V}_{cr,D}$ that

$$(\nabla_h \tilde{y}_h^n, \nabla_h z_h) = (P_0 \tilde{\Phi}_h^n, \nabla_h z_h) + t^2(f, z_h).$$

- (iv) For all $z_h \in \mathbb{V}_{cr,D}$ we have that

$$(\nabla_h[\tilde{y}_h^n - y_h^{n-1}], \nabla_h z_h) = (P_0[\tilde{\Phi}_h^n - \Phi_h^{n-1}], \nabla_h z_h).$$

4.2 Convergence of the iteration

We show that if the time-step size τ is sufficiently small then the iteration is energy decreasing and converges to a stationary point.

Theorem 4.1 (Convergence) *Assume that \mathcal{T}_h is weakly acute. If $\tau \leq C_1 t$ then we have for all $N \geq 1$ that*

$$E_{h,t}(\Phi_h^N, y_h^N) + (\tau/2) \sum_{\ell=1}^N \|\nabla \tilde{d}_t \Phi_h^\ell\|^2 \leq E_{h,t}(\Phi_h^0, y_h^0),$$

where $\tilde{d}_t \Phi_h^\ell = (\tilde{\Phi}_h^\ell - \Phi_h^{\ell-1})/\tau$, and

$$\|\mathcal{I}_h[\Phi_{h,1}^N \cdot \Phi_{h,2}^N]\|_{L^1(\Omega)} \leq C_2 \tau E_{h,t}(\Phi_h^0, y_h^0).$$

The constants C_1, C_2 depend on upper bounds for $\|\nabla \Phi_h^0\|, \|\nabla_h y_h^0\|, \|f\|, \alpha$, and α^{-1} .

Proof Given two sequences (a^n) and (\tilde{a}^n) we write $\tilde{d}_t a^n = (\tilde{a}^n - a^{n-1})/\tau$ in this proof.

(i) *Induction hypothesis* We argue by induction over N and assume that the first estimate of the theorem has been proved for $N - 1$. This is trivially true for $N = 1$ and given $N \geq 1$ we consider $1 \leq n \leq N$ in the following.

(ii) *Elementary bounds* We will repeatedly use the estimates

$$\|P_0 \tilde{\Phi}_h^n\| + \|\nabla \tilde{y}_h^n\| \leq C(1 + \|\nabla \tilde{\Phi}_h^n\|), \quad \|P_0 \Phi_h^n\| + \|\nabla y_h^n\| \leq C(1 + \|\nabla \Phi_h^n\|).$$

(iii) *Local energy inequality* Upon choosing $\Psi_h = \tilde{d}_t \Phi_h^n$ and $z_h = \tilde{d}_t y_h^n$ in the Euler-Lagrange equations related to the minimization problem in Step A, cf. Remark 4.1, we have

$$\begin{aligned} & \|\nabla \tilde{d}_t \Phi_h^n\|^2 + \tilde{d}_t \left(\frac{t^{-2}}{2} \|P_0 \Phi_h^n - \nabla_h y_h^n\|^2 + \frac{\alpha}{2} \|\nabla \Phi_h^n\|^2 - (f, y_h^n) \right) \\ & + \tau \left(\frac{t^{-2}}{2} \|\tilde{d}_t (P_0 \Phi_h^n - \nabla_h y_h^n)\|^2 + \frac{\alpha}{2} \|\tilde{d}_t \nabla \Phi_h^n\|^2 \right) = 0, \end{aligned} \quad (4.2)$$

i.e., $\tau \|\nabla \tilde{d}_t \Phi_h^n\|^2 + E_{h,t}(\tilde{\Phi}_h^n, \tilde{y}_h^n) \leq E_{h,t}(\Phi_h^{n-1}, y_h^{n-1})$.

(iv) *Coarse bound for $\|\nabla \Phi_h^n\|$.* We deduce from (4.2) and the induction hypothesis that

$$\begin{aligned} \frac{\alpha}{2} \|\nabla \tilde{\Phi}_h^n\|^2 & \leq E_{h,t}(\Phi_h^{n-1}, y_h^{n-1}) + (f, \tilde{y}_h^n) \\ & \leq E_{h,t}(\Phi_h^0, y_h^0) + (f, \tilde{y}_h^n) \leq C(1 + t^{-2}) + \frac{\alpha}{4} \|\nabla \tilde{\Phi}_h^n\|^2. \end{aligned}$$

so that we have

$$\|\nabla \tilde{\Phi}_h^n\| \leq Ct^{-1}.$$

(v) *Bound for projection error* Since $\Phi_{h,j}^n(z) = \tilde{\Phi}_{h,j}^n(z)/|\tilde{\Phi}_{h,j}^n(z)|$ and $\tilde{d}_t \Phi_{h,j}^n(z) \cdot \Phi_{h,j}^{n-1}(z) = 0$ for $j = 1, 2$ and every $z \in \mathcal{N}_h$ we have

$$|\Phi_{h,j}^n(z) - \tilde{\Phi}_{h,j}^n(z)| = |\tilde{\Phi}_{h,j}^n(z)| - 1 = (1 + \tau^2 |\tilde{d}_t \Phi_h^n(z)|^2)^{1/2} - 1 \leq (\tau^2/2) |\tilde{d}_t \Phi_h^n(z)|^2.$$

A Sobolev inequality and (2.2) imply

$$\|\tilde{\Phi}_h^n - \Phi_h^n\| \leq C\tau^2 \|\tilde{d}_t \mathcal{I}_h \Phi_h^n\|_{L^4(\Omega)}^2 \leq C\tau^2 \|\tilde{d}_t \nabla \Phi_h^n\|^2,$$

where we also used that $\|\nabla \tilde{d}_t \mathcal{I}_h \Phi_h^n\| \leq \|\nabla \tilde{d}_t \Phi_h^n\|$.

(vi) *Energy of projected iterates* We want to show that

$$E_{h,t}(\Phi_h^n, y_h^n) \leq E_{h,t}(\tilde{\Phi}_h^n, \tilde{y}_h^n) + (\tau/2) \|\tilde{d}_t \nabla \Phi_h^n\|^2. \quad (4.3)$$

By (2.3) we have

$$\|\nabla \Phi_h^n\| \leq \|\nabla \tilde{\Phi}_h^n\|.$$

Using $\|\nabla_h(\tilde{y}_h^n - y_h^n)\| \leq \|\tilde{\Phi}_h^n - \Phi_h^n\|$ we verify with the identity $a^2 - b^2 = (a-b)(a+b)$ that

$$\begin{aligned} & \|P_0\Phi_h^n - \nabla_h y_h^n\|^2 - \|P_0\tilde{\Phi}_h^n - \nabla_h \tilde{y}_h^n\|^2 \\ & \leq \|P_0(\tilde{\Phi}_h^n - \Phi_h^n) - \nabla_h(\tilde{y}_h^n - y_h^n)\|(\|P_0\tilde{\Phi}_h^n - \nabla_h \tilde{y}_h^n\| + \|P_0\Phi_h^n - \nabla_h y_h^n\|) \\ & \leq 2\|\tilde{\Phi}_h^n - \Phi_h^n\|(\|P_0\tilde{\Phi}_h^n\| + \|\nabla_h \tilde{y}_h^n\| + \|P_0\Phi_h^n\| + \|\nabla_h y_h^n\|) \\ & \leq C\tau^2\|\nabla_t \tilde{\Phi}_h^n\|^2(1 + \|\nabla \tilde{\Phi}_h^n\|) \leq C\tau\|\nabla_t \tilde{\Phi}_h^n\|^2\tau(1 + t^{-1}). \end{aligned}$$

Finally, we note that

$$-\int_{\Omega} f y_h^n dx + \int_{\Omega} f \tilde{y}_h^n dx \leq \|f\| \|y_h^n - \tilde{y}_h^n\| \leq C\|f\| \|\Phi_h^n - \tilde{\Phi}_h^n\| \leq C\tau^2\|f\| \|\nabla_t \tilde{\Phi}_h^n\|^2.$$

For $\tau \leq Ct$ the combination of the last three estimates leads to (4.3).

(vii) *Global energy inequality* Using (4.3) in (4.2) shows

$$E_{h,t}(\Phi_h^n, y_h^n) + (\tau/2)\|\nabla_t \tilde{\Phi}_h^n\|^2 \leq E_{h,t}(\Phi_h^{n-1}, y_h^{n-1}),$$

for all $1 \leq n \leq N$ and this implies the induction hypothesis for N and thus the first assertion of the theorem.

(viii) *Almost-orthogonality of column vectors* Since for every $z \in \mathcal{N}_h$ we have $\tilde{d}_t \Phi_{h,1}^n(z) \cdot \Phi_{h,2}^{n-1}(z) + \tilde{d}_t \Phi_{h,2}^n(z) \cdot \Phi_{h,1}^{n-1}(z) = 0$ we deduce that

$$\begin{aligned} & (|\tilde{\Phi}_{h,1}^n(z)|\Phi_{h,1}^n(z)) \cdot (|\tilde{\Phi}_{h,2}^n(z)|\Phi_{h,2}^n(z)) = \tilde{\Phi}_{h,1}^n(z) \cdot \tilde{\Phi}_{h,2}^n(z) \\ & = \Phi_{h,1}^{n-1}(z) \cdot \Phi_{h,2}^{n-1}(z) + \tau^2 \tilde{d}_t \Phi_{h,1}^n(z) \cdot \tilde{d}_t \Phi_{h,2}^n(z) \end{aligned}$$

and thus, since $|\tilde{\Phi}_{h,1}^n(z)|, |\tilde{\Phi}_{h,2}^n(z)| \geq 1$, we deduce with (2.2) that

$$\begin{aligned} \|\mathcal{I}_h[\Phi_{h,1}^n \cdot \Phi_{h,2}^n]\|_{L^1(\Omega)} & \leq \|\mathcal{I}_h[\Phi_{h,1}^{n-1} \cdot \Phi_{h,2}^{n-1}]\|_{L^1(\Omega)} + \tau^2 \|\tilde{d}_t \Phi_{h,1}^n\| \|\tilde{d}_t \Phi_{h,2}^n\| \\ & \leq \|\mathcal{I}_h[\Phi_{h,1}^{n-1} \cdot \Phi_{h,2}^{n-1}]\|_{L^1(\Omega)} + C\tau^2 \|\tilde{d}_t \nabla \Phi_h^n\|^2. \end{aligned}$$

An inductive argument with $\mathcal{I}_h[\Phi_{h,1}^0 \cdot \Phi_{h,2}^0] = 0$ proves the second assertion of the theorem. \square

Remark 4.2 (i) The result of the theorem is based on the estimate

$$E_{h,t}(\Phi_h^n, y_h^n) \leq E_{h,t}(\tilde{\Phi}_h^n, \tilde{y}_h^n) + (\tau/2)\|\tilde{d}_t \nabla \Phi_h^n\|^2$$

which can be monitored during a simulation and used to adjust the time-step size. This is important when the (unknown) constant C_1 in $\tau \leq C_1 t$ is small.

(ii) If \mathcal{T}_h is not weakly acute then we need to assume additionally that $\tau \leq Ch^2$ to derive the same result, cf. [3].

5 Efficient implementation

5.1 Motivation

To motivate an efficient implementation of Step A of the algorithm proposed in the previous section, we discuss the numerical scheme in a semi-discrete setting. Given $\Phi^{n-1} \in H^1(\Omega; \mathbb{R}^{3 \times 2})$ we need to find a minimizing pair $(\tilde{\Phi}^n, \tilde{y}^n) \in H^1(\Omega; \mathbb{R}^{3 \times 2}) \times H^1(\Omega; \mathbb{R}^3)$ for

$$E_t^n(\Phi, y) = \frac{1}{2\tau} \|\nabla(\Phi - \Phi^{n-1})\|^2 + \frac{t^{-2}}{2} \|\Phi - \nabla y\|^2 + \frac{\alpha}{2} \int_{\Omega} |\nabla \Phi|^2 dx - \int_{\Omega} f \cdot y dx$$

subject to the boundary conditions $\tilde{y}^n = y_D$ and $\tilde{\Phi}^n = \Phi_D$ on Γ_D and the pointwise constraint

$$(\tilde{\Phi}^n - \Phi^{n-1})^\top \Phi^{n-1} + \Phi^{n-1, \top} (\tilde{\Phi}^n - \Phi^{n-1}) = 0.$$

The corresponding Euler–Lagrange equations read

$$\begin{aligned} \frac{1}{\tau} (\nabla(\tilde{\Phi}^n - \Phi^{n-1}), \nabla \Psi) + t^{-2} (\tilde{\Phi}^n - \nabla \tilde{y}^n, \Psi) + \alpha (\nabla \tilde{\Phi}^n, \nabla \Psi) &= 0, \\ -t^{-2} (\tilde{\Phi}^n - \nabla \tilde{y}^n, \nabla z) - (f, z) &= 0, \end{aligned} \quad (5.1)$$

for all $\Psi \in H_D^1(\Omega; \mathbb{R}^{3 \times 2})$ and $z \in H_D^1(\Omega; \mathbb{R}^3)$ with $(\Psi - \Phi^{n-1})^\top \Phi^{n-1} + \Phi^{n-1, \top} (\Psi - \Phi^{n-1}) = 0$. Notice that on Γ_N we have $t^{-2} (\tilde{\Phi}^n - \nabla \tilde{y}^n) \nu = 0$. Following Ref. [2] we choose $r^n \in H_D^1(\Omega; \mathbb{R}^3)$ and $p^n \in H^1(\Omega; \mathbb{R}^3)$ with $(\nabla r^n) \nu = 0$ and $(\text{Curl } p^n) \nu = 0$ on Γ_N and $(p^n, 1) = 0$ such that

$$t^{-2} (\tilde{\Phi}^n - \nabla \tilde{y}^n) = -\nabla r^n - \text{Curl } p^n. \quad (5.2)$$

Using that $(\text{Curl } p^n, \nabla z) = 0$ for all $z \in H_D^1(\Omega; \mathbb{R}^3)$ we can simplify the solution of (5.1) as follows:

(i) From (5.2) and the second identity in (5.1) we get for all $\eta \in H_D^1(\Omega; \mathbb{R}^3)$ that

$$(\nabla r^n, \nabla \eta) = (f, \eta).$$

(ii) From (5.2) and the first equation in (5.1) we get for all $\Psi \in H_D^1(\Omega; \mathbb{R}^{3 \times 2})$ with $(\Psi - \Phi^{n-1})^\top \Phi^{n-1} + \Phi^{n-1, \top} (\Psi - \Phi^{n-1}) = 0$ that

$$\frac{1}{\tau} (\nabla(\tilde{\Phi}^n - \Phi^{n-1}), \nabla \Psi) - (\text{Curl } p^n, \Psi) + \alpha (\nabla \tilde{\Phi}^n, \nabla \Psi) = (\nabla r^n, \Psi).$$

(iii) Testing (5.2) with $\text{Curl } q$ for $q \in H^1(\Omega; \mathbb{R}^3)$ such that $(\text{Curl } q) \nu = 0$ on Γ_N and $(q, 1) = 0$ yields that

$$(\tilde{\Phi}^n, \text{Curl } q) + t^2 (\text{Curl } p^n, \text{Curl } q) = 0.$$

(iv) Testing (5.2) with ∇z for $z \in H_D^1(\Omega; \mathbb{R}^3)$ yields that

$$(\nabla y^n, \nabla z) = (\tilde{\Phi}^n, \nabla z) + t^2(\nabla r^n, \nabla z).$$

Notice that the formulation in (i) can be solved individually, that (ii)–(iii) defines a saddle-point problem with penalty term (which in general is owing to certain boundary terms not the variational derivative of a quadratic energy functional), and that (iv) can be solved once the solutions of (i)–(iii) have been computed. We also observe that r^n is independent of n and that y^n is not required in the solution of (ii)–(iii), hence the formulation (ii)–(iii) can be iterated without solving (i) and (iv).

5.2 Discrete realization

The reformulation described above leads to the following implementation of the iterative algorithm which we stop if the magnitude of the rate of decrease of the energy is smaller than the prescribed parameter $\varepsilon_{stop} > 0$.

Step 0. Choose a parameter $\varepsilon_{stop} > 0$, a time-step size $\tau > 0$, a regular triangulation \mathcal{T}_h , a parameter $t > 0$, and $\Phi_h^0 \in \mathbb{V}_{mini}^2$ with $\Phi_h^0(z) = \Phi_D(z)$ for all $z \in \mathcal{N}_h \cap \Gamma_D$ and $\Phi_h^0(z)^\top \Phi_h^0(z) = I_2$ for all $z \in \mathcal{N}_h$. Set $n = 1$.

Step 1. Compute $r_h \in \mathbb{V}_{cr,D}$ such that

$$(\nabla_h r_h, \nabla_h \eta_h) = (f, \eta_h)$$

for all $\eta_h \in \mathbb{V}_{cr,D}$.

Step 2. Compute $\tilde{d}_t \Phi_h^n \in \mathbb{W}_{mini,D}[\Phi_h^{n-1}]$ and $p_h^n \in \mathring{\mathbb{Q}}_{p1,N}$ such that

$$\begin{aligned} (\nabla \tilde{d}_t \Phi_h^n, \nabla \Psi_h) + \alpha(\nabla(\tau \tilde{d}_t \Phi_h^n + \Phi_h^{n-1}), \nabla \Psi_h) - (\text{Curl} p_h^n, \Psi_h) &= (\nabla_h r_h, \Psi_h), \\ -\tau(\tilde{d}_t \Phi_h^n, \text{Curl} q_h) - t^2(\text{Curl} p_h^n, \text{Curl} q_h) &= (\Phi_h^{n-1}, \text{Curl} q_h) \end{aligned}$$

for all $\Psi_h \in \mathbb{W}_{mini,D}[\Phi_h^{n-1}]$ and $q_h \in \mathring{\mathbb{Q}}_{p1,N}$.

Step 3. Define $\Phi_h^n = \mathcal{I}_B \tilde{\Phi}_h^n + \hat{\Phi}_h^n \in \mathbb{V}_{mini}^2$, where $\hat{\Phi}_h^n = [\hat{\Phi}_{h,1}^n, \hat{\Phi}_{h,2}^n] \in \mathbb{V}_{p1}^2$ is defined by setting for all $z \in \mathcal{N}_h$

$$\hat{\Phi}_{h,1}^n(z) = \frac{\Phi_{h,1}^{n-1}(z) + \tau \tilde{d}_t \Phi_{h,1}^n(z)}{|\Phi_{h,1}^{n-1}(z) + \tau \tilde{d}_t \Phi_{h,1}^n(z)|}, \quad \hat{\Phi}_{h,2}^n(z) = \frac{\Phi_{h,2}^{n-1}(z) + \tau \tilde{d}_t \Phi_{h,2}^n(z)}{|\Phi_{h,2}^{n-1}(z) + \tau \tilde{d}_t \Phi_{h,2}^n(z)|}.$$

Step 4. Compute $y_h^n \in \mathbb{V}_{cr}$ with $y_h^n(z_E) = y_D(z_E)$ for all $E \in \mathcal{E}_h \cap \Gamma_D$ and

$$(\nabla_h y_h^n, \nabla_h z_h) = (P_0 \Phi_h^n, \nabla_h z_h) + t^2(\nabla_h r_h, \nabla_h z_h)$$

for all $z_h \in \mathbb{V}_{cr,D}$.

Step 5. Stop if $E_{h,t}(\Phi_h^n, y_h^n) - E_{h,t}(\Phi_h^{n-1}, y_h^{n-1}) \geq -\tau \varepsilon_{stop}$.

Step 6. Set $n = n + 1$ and go to Step 2.

Remark 5.1 (i) The projection $P_0\Phi_h$ guarantees that there exists a discrete Helmholtz decomposition $t^{-2}(P_0\tilde{\Phi}_h^n - \nabla_h\tilde{y}_h^n) = -\nabla_h r_h^n - \text{Curl} p_h^n$, cf. [2].

(ii) The degrees of freedom related to the functions in $\mathcal{B}^3(\mathcal{T}_h)$ can be eliminated from the equations since the related stiffness matrix decouples owing to (2.1) and can be explicitly inverted, i.e., Step 2 in matrix-vector notation reads

$$\begin{bmatrix} S_{P1} + \tau L_{P1} & 0 & -C_{P1}^\top \\ 0 & S_B + \tau L_B & -C_B^\top \\ -\tau C_{P1} & -\tau C_B & -t^2 s_{p1} \end{bmatrix} \begin{bmatrix} \tilde{d}_t \Phi_{P1} \\ \tilde{d}_t \Phi_B \\ p \end{bmatrix} = \begin{bmatrix} G_{P1}r - L_{P1}\Phi_{P1}^{n-1} \\ G_B r - L_B\Phi_B^{n-1} \\ C_{P1}\Phi_{P1}^{n-1} + C_B\Phi_B^{n-1} \end{bmatrix}$$

and using that $\tilde{d}_t \Phi_B = X_B^{-1}(C_B^\top p + G_B r - L_B\Phi_B^{n-1})$, where $X_B = (S_B + \tau L_B)$, this is equivalent to the system

$$\begin{bmatrix} S_{P1} + \tau L_{P1} & -C_{P1}^\top \\ -\tau C_{P1} & -\tau C_B X_B^{-1} C_B^\top - t^2 s_{p1} \end{bmatrix} \begin{bmatrix} \tilde{d}_t \Phi_{P1} \\ p \end{bmatrix} = \begin{bmatrix} G_{P1}r - L_{P1}\Phi_{P1}^{n-1} \\ C_{P1}\Phi_{P1}^{n-1} + C_B\Phi_B^{n-1} + b'_B \end{bmatrix}$$

with $b'_B = \tau X_B^{-1}(G_B r - L_B\Phi_B^{n-1})$. We have $L_{P1} = \alpha S_{P1}$ and $L_B = \alpha S_B$.

(iii) In our implementation the nodal constraints included in the definition of the set $\mathbb{W}_{\text{mini,D}}[\Phi_h^{n-1}]$ in Step 2 of the algorithm are enforced via Lagrange multipliers.

(iv) The inf-sup condition can not be expected to hold for the linear system of equations in Step 2 of the algorithm, i.e., for $\Psi \in \mathbb{R}^{3 \times 2}$ there does in general not exist $\Phi \in H^1(\Omega; \mathbb{R}^{3 \times 2})$ with $\text{curl} \Phi = F$ for given $F \in L^2(\Omega; \mathbb{R}^3)$ such

that $\Phi^\top \Psi + \Psi^\top \Phi = 0$. The situation $\Psi = \begin{bmatrix} 1 & 0 & 0 \\ 0 & 1 & 0 \end{bmatrix}^\top$ and $F = (0, 0, f)^\top$

corresponds to small displacements and a vertical load and in this case the inf-sup condition holds, cf. [2]. Nevertheless, a unique discrete solution always exists in Step 2.

(v) The decrease of the energy $E_{h,t}(\Phi_h^n, y_h^n) \leq E_{h,t}(\Phi_h^{n-1}, y_h^{n-1})$ guaranteed by Theorem 4.1 for τ sufficiently small can be monitored during the iteration. If this energy decrease is violated the time-step size should be decreased.

6 Numerical experiments

To illustrate the practical performance of our algorithm we study three prototypical specifications of the model problem. These are defined by vertical loads with a fixed part of the boundary of the plate and compressive boundary conditions in the absence of an exterior body force. In all of our experiments we employed triangulations $\mathcal{T}_h = \mathcal{T}_\ell$ determined by a positive integer ℓ that consist of halved squares with edge-lengths $\hat{h} = 2^{-\ell}$ and diameters $h = \sqrt{2}\hat{h}$. Motivated by Remark 3.2 we set $t = \hat{h}^{1/2}/4$ and defined $\tau = \hat{h}/4$ so that the conditions of Theorems 3.1 and 4.1 are satisfied. The stopping criterion of our algorithm was specified by $\varepsilon_{\text{stop}} = 1.0 \times 10^{-3}$. To display the

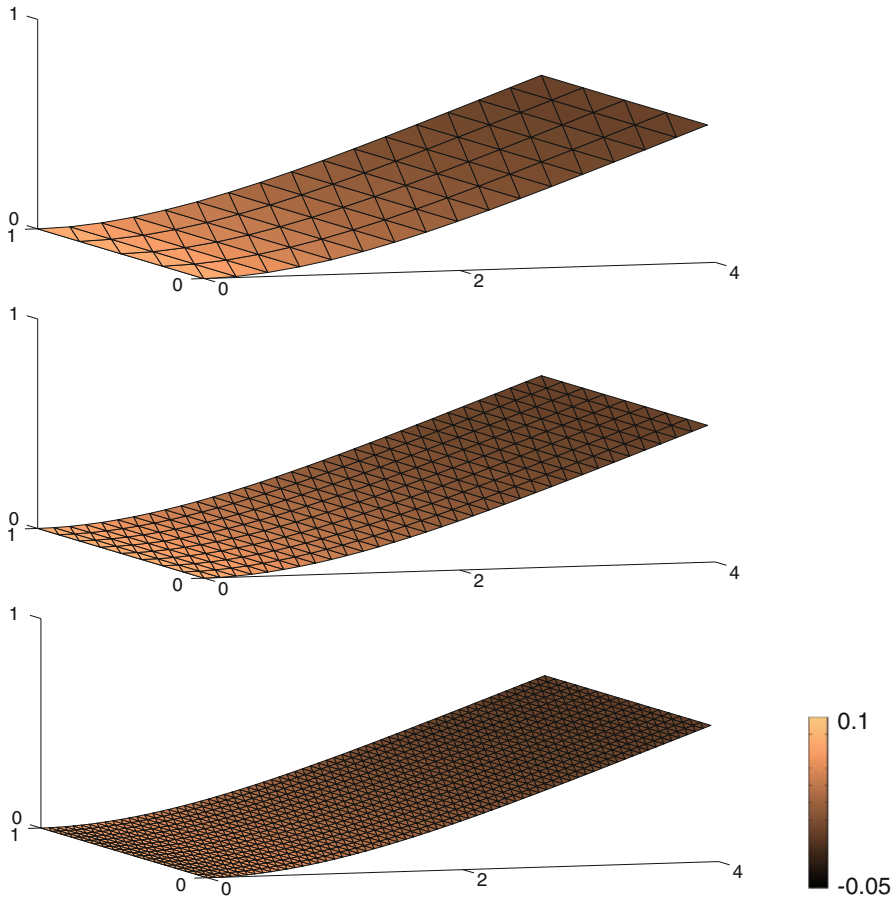


Fig. 1 Deformations of a clamped 4×1 plate for a uniform vertical load on different uniform triangulations. The deformations are colored by the discrete mean curvature H_h (color figure online)

possibly discontinuous discrete displacement $y_h \in \mathbb{V}_{cr}$ we employed an L^2 projection of y_h onto the respective C^0 -conforming finite element space \mathbb{V}_{p1} .

6.1 Vertical load on a rectangular plate

The first problem considers a rectangular plate that is clamped on one side and subject to a vertical load.

Example 6.1 Let $\Omega = (0, 4) \times (0, 1)$, $\Gamma_D = \{0\} \times [0, 1]$, $\alpha = 1$, $y_D(x) = (x, 0)^\top$ and $b_D(x) = (0, 0, 1)^\top$ for $x \in \Gamma_D$, and $f(x) = c_f(0, 0, 1)^\top$ for $x \in \Omega$ with $c_f = 2.5 \times 10^{-2}$.

For $\ell = 2, 3, 4$ we plotted in Fig. 1 the outputs of our approximation scheme. The deformed plate is colored by the discrete mean curvature $H_h = (1/2)\text{tr}II_h$ for the

Table 1 Iteration numbers, computed energy, deviation of the discrete first fundamental form from I_2 , norm of the discrete Gaussian curvature, and inner product of the column vectors of Φ_h for the iteration of the iterative algorithm on triangulations with different mesh-sizes for a vertical load on a clamped rectangular plate

\hat{h}	N_{iter}	$E_{h,t}(\Phi_h, y_h)$	$\ \delta_I\ _{L^1(\Omega)}$	$\ K_h\ _{L^1(\Omega)}$	$\ \mathcal{I}_h[\Phi_{h,1} \cdot \Phi_{h,2}]\ _{L^1(\Omega)}$
2^{-2}	29	-1.543×10^{-2}	7.304×10^{-4}	6.035×10^{-6}	1.778×10^{-6}
2^{-3}	56	-1.536×10^{-2}	3.656×10^{-4}	1.498×10^{-6}	2.463×10^{-7}
2^{-4}	110	-1.532×10^{-2}	1.890×10^{-4}	3.669×10^{-7}	3.208×10^{-8}
2^{-5}	219	-1.531×10^{-2}	9.717×10^{-5}	9.037×10^{-8}	4.117×10^{-9}

piecewise constant approximation of the second fundamental form defined by

$$II_h = -(\nabla \mathcal{I}_h[\Phi_{h,1} \times \Phi_{h,2}])^\top \nabla_h y_h.$$

As initial guesses we chose the compatible pairs $\Phi_h^0(x) = \begin{bmatrix} 1 & 0 & 0 \\ 0 & 1 & 0 \end{bmatrix}^\top$ and $y_h^0(x) = (x, 0)^\top$ for $x \in \Omega$. We observe that the deformations do not differ significantly for the different mesh-sizes and that the deformations can not be approximated as graphs of functions defined on Ω . In the second column of Table 1 we displayed for $\ell = 2, 3, 4, 5$ the number of iterations carried out by our algorithm before termination. As expected, the number of time steps needed to satisfy the stopping criterion grows linearly. The computed energy $E_{h,t}(\Phi_h, y_h)$ of the output is shown in the third column and it increases as the mesh-size \hat{h} decreases. The failure of being an exact isometry, i.e., the L^1 norm of the elementwise constant function

$$\delta_I = (\nabla_h y_h)^\top \nabla_h y_h - I_2,$$

is shown in the fourth column of Table 1 and we observe that this quantity decreases nearly linearly to zero. We also displayed the L^1 norm of an elementwise constant approximation of the Gaussian curvature defined by $K_h = \det II_h$. The experimental results show that this quantity decays almost quadratically to zero as h approaches zero. As is guaranteed by Theorem 4.1, the column vectors of the computed approximations Φ_h are nearly orthogonal and this is confirmed by the numbers displayed in the last column of Table 1.

6.2 Vertical load on a square-shaped plate

To illustrate the performance of our algorithm when the profile of the deformation is not one-dimensional in the direction of one of the coordinate axes, we employ a square-shaped plate that is clamped on two nonparallel sides and a load as in Example 6.1.

Example 6.2 Let $\Omega = (0, 4) \times (0, 4)$, $\Gamma_D = \{0\} \times [0, 4] \cup [0, 4] \times \{4\}$, $\alpha = 1$, $y_D(x) = (x, 0)^\top$ and $b_D(x) = (0, 0, 1)^\top$ for all $x \in \Gamma_D$, and $f(x) = c_f(0, 0, 1)^\top$ for $x \in \Omega$ with $c_f = 2.5 \times 10^{-2}$.

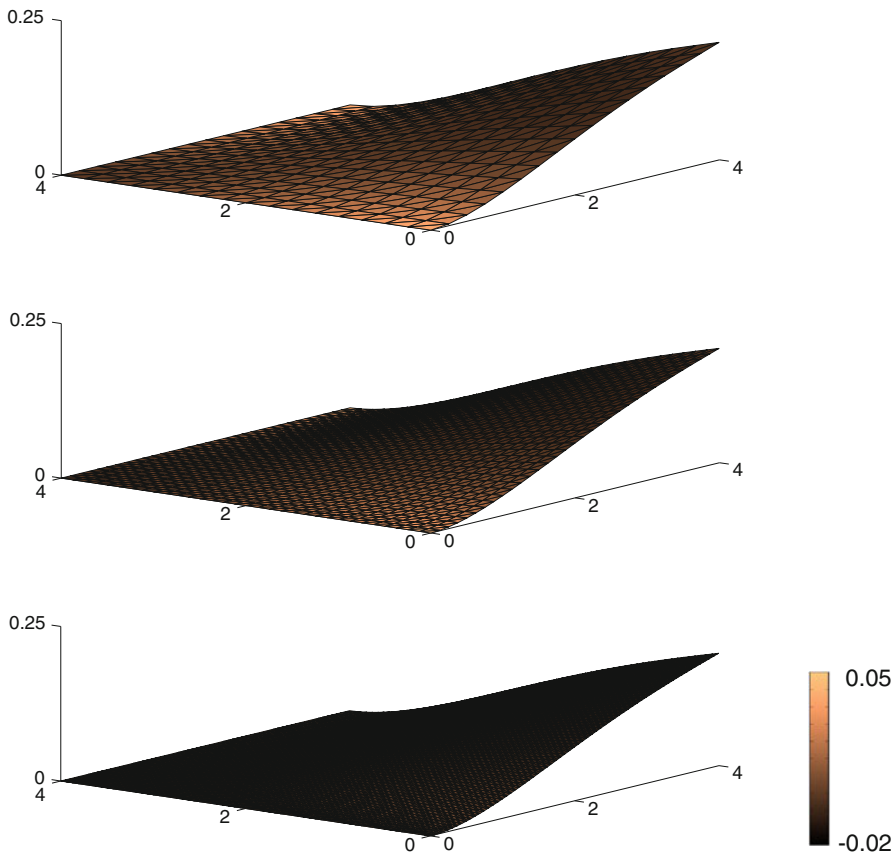


Fig. 2 Deformations of a clamped 4×4 plate for a uniform vertical load on different uniform triangulations coloured by discrete mean curvature (color figure online)

We used the same initial pairs (Φ_h^0, y_h^0) as in the previous experiment. The outputs of our algorithm are for three different triangulations defined by $\ell = 2, 3, 4$ shown in Fig. 2 and we observe a nontrivial large deformation. We note that the employed triangulations are such that the diagonals of halved squares are orthogonal to the direction $(1, 1)$ so that the triangulations do not lead to an artificial improvement of the computed solution. We also tested the algorithm with triangulations for which the diagonals of halved squares were parallel to $(1, 1)$ and observed nearly the same results. Table 2 displays the iteration numbers, the computed energies, the deviation of the discrete first fundamental form from the identity matrix, the L^1 norm of the discrete Gaussian curvature, and the L^1 norm of the inner product of the column vectors of the output Φ_h for different mesh-sizes. We see that in this experiment the discrete first fundamental form approaches the unity matrix only very slowly and also the discrete Gaussian curvature decreases slowly as the mesh-size becomes smaller.

Table 2 Iteration numbers, computed energy, deviation of the discrete first fundamental form from I_2 , norm of the discrete Gaussian curvature, and inner product of the column vectors of Φ_h for the iteration of the iterative algorithm on triangulations with different mesh-sizes for a vertical load on a clamped square-shaped plate

\hat{h}	N_{iter}	$E_{h,t}(\Phi_h, y_h)$	$\ \delta_I\ _{L^1(\Omega)}$	$\ K_h\ _{L^1(\Omega)}$	$\ \mathcal{I}_h[\Phi_{h,1} \cdot \Phi_{h,2}]\ _{L^1(\Omega)}$
2^{-2}	26	-1.009×10^{-2}	5.444×10^{-3}	2.234×10^{-3}	2.551×10^{-4}
2^{-3}	49	-9.864×10^{-3}	5.138×10^{-3}	2.162×10^{-3}	1.168×10^{-4}
2^{-4}	96	-9.721×10^{-3}	5.007×10^{-3}	2.130×10^{-3}	5.550×10^{-5}
2^{-5}	185	-9.545×10^{-3}	4.776×10^{-3}	2.043×10^{-3}	2.672×10^{-5}

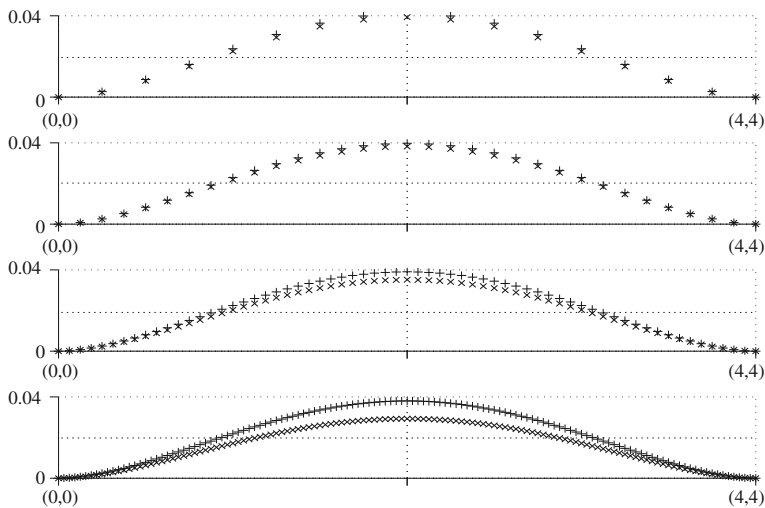


Fig. 3 Third component of the discrete deformations for $\ell = 2, 3, 4, 5$ (top to bottom) with $t = \hat{h}^{1/2}/4$ (plusses) and $t = \hat{h}/4$ (crosses) along the diagonal $\{(x_1, x_2) \in \Omega : x_1 = x_2\}$ for a vertical load on a clamped 4×4 plate

The relative change of the area of the deformed plate is approximately $5.0 \times 10^{-3}/16.0 \approx 0.03\%$.

For clamped boundary conditions on $\Gamma_D \subset \partial\Omega$ we expect that any isometric deformation coincides with the identity inside the convex hull of Γ_D . Hence, in Example 6.2 the third component of the discrete deformations y_h should converge to zero in the region above the diagonal $\{(x_1, x_2) \in \Omega : x_1 = x_2\}$. In Fig. 3 we plotted the third component of the approximate deformations along this diagonal for different mesh-sizes and for the relations $t = \hat{h}^{1/2}/4$ as well as for $t = \hat{h}/4$. We observe that the curves slowly converge to zero and that the curves related to the smaller value of t lie below the ones for the larger values. Table 3 shows the maxima of the curves and we see that these values decrease slowly as the mesh-size decreases. The numbers imply that we have a relative approximation error in L^∞ of about 10% and that a choice $t \sim \hat{h}^{1-\varepsilon}$ for some small parameter $\varepsilon > 0$ may be preferable over $t \sim \hat{h}^{1/2}$ in this example.

Table 3 Maximum value of the third component of the discrete deformations along the diagonal $\{(x_1, x_2) \in \Omega : x_1 = x_2\}$ for a vertical load on a 4×4 plate

t	$\hat{h} = 2^{-2}$	$\hat{h} = 2^{-3}$	$\hat{h} = 2^{-4}$	$\hat{h} = 2^{-5}$
$\hat{h}^{1/2}/4$	4.110×10^{-2}	3.973×10^{-2}	3.902×10^{-2}	3.804×10^{-2}
$\hat{h}/4$	3.931×10^{-2}	3.815×10^{-2}	3.510×10^{-2}	2.924×10^{-2}

6.3 Compression of a strip

We next study compressive boundary conditions on part of the boundary of a rectangular plate. A small vertical load selects one of two possible solutions related to the symmetry in vertical direction of the problem for $f = 0$.

Example 6.3 Let $\Omega = (-2, 2) \times (0, 1)$, $\Gamma_D = \{-2, 2\} \times [0, 1]$, $\alpha = 1$, $f(x) = c_f(0, 0, 1)^\top$ with $c_f = 1.0 \times 10^{-5}$ for $x \in \Omega$, $b_D = (0, 0, 1)^\top$ on Γ_D , and

$$y_D(x) = (x_1 \pm a, x_2, 0)^\top$$

for $(x_1, x_2) \in \Gamma_D$ with $x_1 = \mp 2$. We set $a = 1.4$.

To start the iteration we set $\Phi_h^0 = \begin{bmatrix} 1 & 0 & 0 \\ 0 & 1 & 0 \end{bmatrix}^\top$ and defined the initial deformation for $x = (x_1, x_2) \in \Omega$ by

$$y_h^0(x) = \begin{cases} (x_1 + a, x_2, 0), & -2 \leq x_1 \leq -a, \\ (0, x_2, x_1 + a), & -a \leq x_1 \leq 0, \\ (0, x_2, -x_1 + a), & 0 \leq x_1 \leq a, \\ (x_1 - a, x_2, 0), & a \leq x_1 \leq 2. \end{cases}$$

We note that this choice of initial guesses is incompatible in the sense that $\|P_0\Phi_h^0 - \nabla_h y_h^0\| \neq 0$. Owing to this possibly suboptimal choice of initial values we found that our choice of the time-step size $\tau = \hat{h}/4$ was almost optimal, i.e., for larger time-steps we did not observe convergence of the iteration for the tested mesh-sizes. The outputs for different mesh-sizes are displayed in Fig. 4 and we observe large curvatures along the line $x_1 = 0$. The computed energies, the iteration numbers, the deviation of the discrete first fundamental form from the identity matrix, the L^1 norm of the discrete Gaussian curvature, and the inner products of the column vectors of Φ_h are displayed in Table 4. The displayed numbers reveal that a large number of iterations is required to approximate a stationary point, that the minimal energies decrease as the mesh-size decreases in this experiment, and that the approximation error for the first fundamental form is nearly linear for $\ell \geq 3$. The L^1 norm of the discrete Gaussian curvature is very small and decays quadratically to zero.

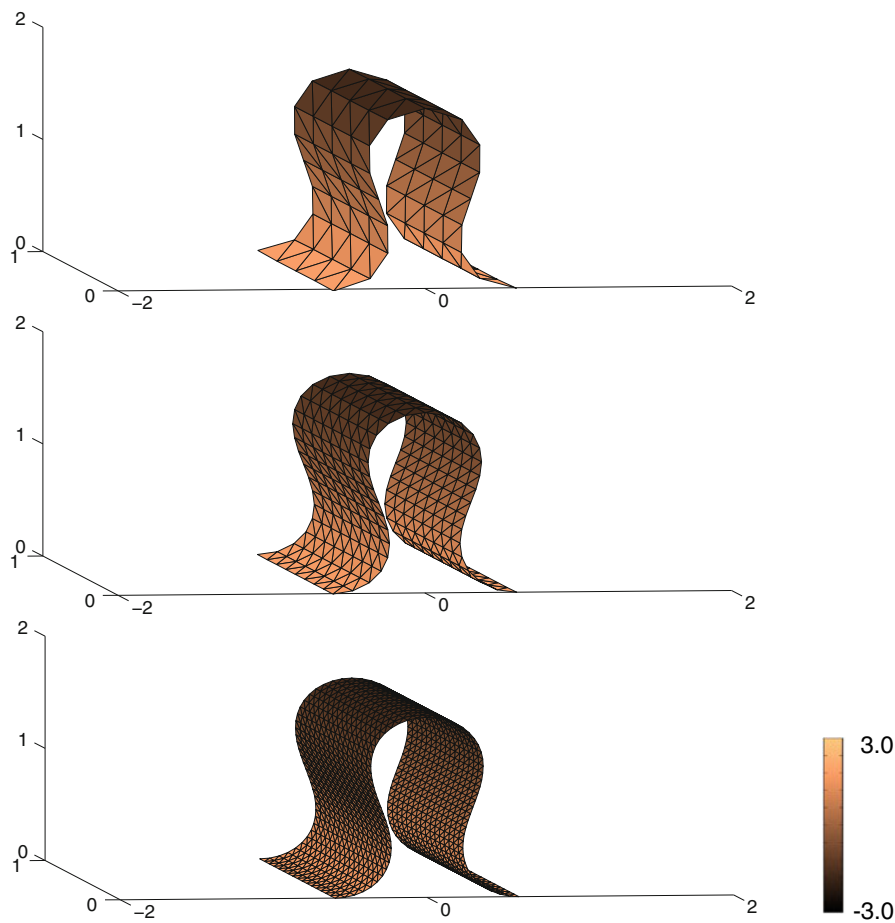


Fig. 4 Numerical solutions for 70.0 % compression of a 4×1 plate on triangulations with different mesh-sizes. The deformations are colored by the discrete mean curvature H_h (color figure online)

Table 4 Iteration numbers, computed energy, deviation of the first fundamental form from identity, norm of the discrete Gaussian curvature, and inner product of the column vectors of Φ_h for the iteration of the iterative algorithm on triangulations with different mesh-sizes for compression

\hat{h}	N_{iter}	$E_{h,t}(\Phi_h, y_h)$	$\ \delta_I\ _{L^1(\Omega)}$	$\ K_h\ _{L^1(\Omega)}$	$\ \mathcal{I}_h[\Phi_{h,1} \cdot \Phi_{h,2}]\ _{L^1(\Omega)}$
2^{-2}	115	1.892	1.857×10^{-1}	2.798×10^{-7}	9.614×10^{-9}
2^{-3}	194	2.713	1.698×10^{-1}	7.173×10^{-8}	8.003×10^{-10}
2^{-4}	357	3.295	1.052×10^{-1}	1.672×10^{-8}	8.121×10^{-11}
2^{-5}	684	3.619	5.753×10^{-2}	4.045×10^{-9}	1.159×10^{-11}

Acknowledgments The author acknowledges support by the DFG through the Collaborative Research Center (SFB) 611 *Singular Phenomena and Scaling in Mathematical Models*.

Appendix A: Auxiliary results

A.1 Elementary differential geometry

Given a parametrized surface $y : \Omega \rightarrow \mathbb{R}^3$ the first fundamental form is given by $g_{ij} = \partial_i y \cdot \partial_j y$ and the second fundamental form by $h_{ij} = \partial_i b \cdot \partial_j y = -b \cdot \partial_i \partial_j y$, where $b = \partial_1 y \times \partial_2 y$. The inverse of g has the entries g^{ij} . The Gaussian curvature is the determinant of the Weingarten map $L = (\sum_k h_{ik} g^{kj})$ and given by $K = \det h_{ij} / \det g_{ij}$. The mean curvature is half of the trace of L and given by $H = (h_{11} g_{22} - 2h_{12} g_{12} + h_{22} g_{11}) / (2 \det g_{ij})$. If the parametrization is an isometry, i.e., if $g_{ij} = \delta_{ij}$, then Gauss's *theorema egregium* implies $K = 0$. Moreover, we have $\text{tr} II = \text{tr} L = 2H$ and

$$\begin{aligned} |II|^2 &= \sum_{i,j} h_{ij}^2 = h_{11}^2 + h_{22}^2 + 2h_{12}^2 = (h_{11} + h_{22})^2 - 2h_{11}h_{22} + 2h_{12}^2 \\ &= 4H^2 - 2K = 4H^2. \end{aligned}$$

For a C^2 isometry with $|\partial_j y|^2 = 1$, $j = 1, 2$, and $\partial_1 y \cdot \partial_2 y = 0$ we deduce that $\partial_1^2 y \cdot \partial_1 y = 0$ and $\partial_1^2 y \cdot \partial_2 y = -\partial_1 y \cdot \partial_1 \partial_2 y = 0$. Analogously, we verify that $\partial_2^2 y \cdot \partial_1 y = -\partial_2 y \cdot \partial_1 \partial_2 y = 0$ and $\partial_2^2 y \cdot \partial_2 y = 0$ so that $-\Delta y = \beta b$. Since $-\Delta y \cdot b = \text{tr} II = 2H$ we verify that $-\Delta y = 2Hb$. The vectors $(\partial_1 y, \partial_2 y, b)$ form an orthonormal basis of \mathbb{R}^3 for every $x \in \Omega$ so that $|\partial_i \partial_j y| = |\partial_i \partial_j y \cdot b|$ and hence $|D^2 y|^2 = \sum_{i,j} |\partial_i \partial_j y \cdot b|^2 = |II|^2$.

A.2 Proof of (2.3)

Given a weakly acute triangulation \mathcal{T}_h we have for the entries $k_{zy} = (\nabla \varphi_z, \nabla \varphi_y)$ of the stiffness matrix that $k_{zy} \leq 0$ if $z \neq y$ for all $z, y \in \mathcal{N}_h$. The symmetry $k_{zy} = k_{yz}$ and the identity $\sum_{y \in \mathcal{N}_h} k_{zy} = 0$ for all $z \in \mathcal{N}_h$ show

$$\begin{aligned} \|\nabla v_h\|^2 &= \frac{1}{2} \sum_{z,y \in \mathcal{N}_h} k_{zy} v_h(z) \cdot (v_h(y) - v_h(z)) + \frac{1}{2} \sum_{z,y \in \mathcal{N}_h} k_{zy} v_h(y) \cdot (v_h(z) - v_h(y)) \\ &= -\frac{1}{2} \sum_{z,y \in \mathcal{N}_h} k_{zy} |v_h(z) - v_h(y)|^2. \end{aligned}$$

The assertion follows from the fact that the mapping $x \mapsto x/|x|$ is Lipschitz continuous with constant 1 in $\{x \in \mathbb{R}^3 : |x| \geq 1\}$.

A.3 Proof of Lemma 2.1

A discrete Poincaré inequality shows that $\|y_h\| \leq C$ and hence there exists $y \in L^2(\Omega; \mathbb{R}^3)$ with (after extraction of a subsequence) $y_h \rightharpoonup y$ in L^2 . Since $\|\nabla_h y_h\| \leq C$ there exists $\xi \in L^2(\Omega; \mathbb{R}^{3 \times 2})$ such that (after extraction of another subsequence)

$\nabla_h y_h \rightharpoonup \xi$ in L^2 . We have, using that $\int_E [y_h] ds = 0$ for all $E \in \mathcal{E}_h$ and that the (row-wise applied) Fortin interpolant $I_F \Psi$ of $\Psi \in C_0^\infty(\Omega; \mathbb{R}^{3 \times 2})$ on the Raviart–Thomas finite element space, cf. [10], satisfies that $(I_F \Psi)v|_E$ is constant on each $E \in \mathcal{E}_h$, that

$$\begin{aligned} \int_{\Omega} \nabla_h y_h : \Psi dx &= - \int_{\Omega} y_h \cdot \operatorname{div} \Psi dx + \sum_{E \in \mathcal{E}_h} \int_E [y_h] \cdot ([\Psi - I_F \Psi]v) ds \\ &= - \int_{\Omega} y_h \cdot \operatorname{div} \Psi dx + \int_{\Omega} \nabla_h y_h : [\Psi - I_F \Psi] dx + \int_{\Omega} y_h \cdot \operatorname{div} [\Psi - I_F \Psi] dx. \end{aligned}$$

Since the last two terms on the right-hand side converge to zero as $h \rightarrow 0$ we deduce that $\xi = \nabla y$. The fact that $y|_{\Gamma_D} = y_D$ follows from an elementwise integration by parts as above provided that $y_h \rightarrow y$ in $L^2(\Gamma_D)$.

References

1. Alouges, F.: A new algorithm for computing liquid crystal stable configurations: the harmonic mapping case. *SIAM J. Numer. Anal.* **34**(5), 1708–1726 (1997)
2. Arnold, D.N., Falk, R.S.: A uniformly accurate finite element method for the Reissner–Mindlin plate. *SIAM J. Numer. Anal.* **26**(6), 1276–1290 (1989)
3. Barrett, J.W., Bartels, S., Feng, X., Prohl, A.: A convergent and constraint-preserving finite element method for the p -harmonic flow into spheres. *SIAM J. Numer. Anal.* **45**(3), 905–927 (2007). (electronic)
4. Barrett, J.W., Garcke, H., Nürnberg, R.: On the variational approximation of combined second and fourth order geometric evolution equations. *SIAM J. Sci. Comput.* **29**(3), 1006–1041 (2007). (electronic)
5. Barrett, J.W., Garcke, H., Nürnberg, R.: Parametric approximation of Willmore flow and related geometric evolution equations. *SIAM J. Sci. Comput.* **31**(1), 225–253 (2008)
6. Bartels, S.: Stability and convergence of finite-element approximation schemes for harmonic maps. *SIAM J. Numer. Anal.* **43**(1), 220–238 (2005). (electronic)
7. Bartels, S.: Approximation of large bending isometries with discrete Kirchhoff triangles. *SIAM J. Numer. Anal.* (2013) (accepted)
8. Bonito, A., Nochetto, R.H., Pauletti, M.S.: Parametric FEM for geometric biomembranes. *J. Comput. Phys.* **229**(9), 3171–3188 (2010)
9. Brenner, S.C., Scott, L.R.: The mathematical theory of finite element methods. Springer, New York (2008)
10. Brezzi, F., Fortin, M.: Mixed and hybrid finite element methods. In: Series in Computational Mathematics, vol. 15. Springer, New York (1991)
11. Clarenz, U., Diewald, U., Dziuk, G., Rumpf, M., Rusu, R.: A finite element method for surface restoration with smooth boundary conditions. *Comput. Aided Geom. Des.* **21**(5), 427–445 (2004)
12. Conti, S., Maggi, F.: Confining thin elastic sheets and folding paper. *Arch. Ration. Mech. Anal.* **187**(1), 1–48 (2008)
13. Deckelnick, K., Dziuk, G., Elliott, C.M.: Computation of geometric partial differential equations and mean curvature flow. *Acta Numer.* **14**, 139–232 (2005)
14. Du, Q., Liu, C., Ryham, R., Wang, X.: A phase field formulation of the Willmore problem. *Nonlinearity* **18**(3), 1249–1267 (2005)
15. Du, Q., Liu, C., Wang, X.: A phase field approach in the numerical study of the elastic bending energy for vesicle membranes. *J. Comput. Phys.* **198**(2), 450–468 (2004)
16. Dziuk, G.: Computational parametric Willmore flow. *Numer. Math.* **111**(1), 55–80 (2008)
17. Elliott, C.M., Stinner, B.: Modeling and computation of two phase geometric biomembranes using surface finite elements. *J. Comput. Phys.* **229**(18), 6585–6612 (2010)

18. Friesecke, G., James, R.D., Müller, S.: The Föppl–von Kármán plate theory as a low energy Γ -limit of nonlinear elasticity. *C. R. Math. Acad. Sci. Paris* **335**(2), 201–206 (2002)
19. Friesecke, G., James, R.D., Müller, S.: A theorem on geometric rigidity and the derivation of nonlinear plate theory from three-dimensional elasticity. *Comm. Pure Appl. Math.* **55**(11), 1461–1506 (2002)
20. Friesecke, G., James, R.D., Müller, S.: A hierarchy of plate models derived from nonlinear elasticity by gamma-convergence. *Arch. Ration. Mech. Anal.* **180**(2), 183–236 (2006)
21. Hornung, P.: Approximation of flat $W^{2,2}$ isometric immersions by smooth ones. *Arch. Ration. Mech. Anal.* **199**(3), 1015–1067 (2011)
22. Hornung, P.: Euler–Lagrange equation and regularity for flat minimizers of the Willmore functional. *Comm. Pure Appl. Math.* **64**(3), 367–441 (2011)
23. Hornung, P.: Fine level set structure of flat isometric immersions. *Arch. Ration. Mech. Anal.* **199**(3), 943–1014 (2011)
24. Hornung, P.: Personal communication (2012)
25. Kirchhoff, G.R.: Über das Gleichgewicht und die Bewegung einer elastischen Scheibe. *J. Reine Angew. Math.* **40**, 51–88 (1850)
26. Pakzad, M.R.: On the Sobolev space of isometric immersions. *J. Differ. Geom.* **66**(1), 47–69 (2004)
27. Wardetzky, M., Bergou, M., Harmon, D., Zorin, D., Grinspun, E.: Discrete quadratic curvature energies. *Comput. Aided Geom. Des.* **24**(8–9), 499–518 (2007)
28. Willmore, T.J.: Total curvature in Riemannian geometry. In: *Ellis Horwood Series: Mathematics and its Applications*. Ellis Horwood Ltd, Chichester (1982)